View Article Online
View Journal

Dalton Transactions

An international journal of inorganic chemistry

Accepted Manuscript

This article can be cited before page numbers have been issued, to do this please use: J. Kim, C. G. Kim, J. Lee and S. Huh, *Dalton Trans.*, 2026, DOI: 10.1039/D6DT00489J.

ROYAL SOCIETY OF CHEMISTRY

rsc.li/dalton

View Article Online
DOI: 10.1039/D6DT00489J

COMMUNICATION

$[Ru(bpy)_2(dppz)]^{2+}$ encapsulated isostructural In-MOFs: a comparative study of their photoluminescence and photoredox catalytic activities

Received 00th January 20xx,
Accepted 00th January 20xx

DOI: 10.1039/x0xx00000x

Jongseo Kim,† Chan Gu Kim,† Juwon Lee and Seong Huh*

The large cationic $[Ru(bpy)_2(dppz)]^{2+}$ complex was encapsulated within the channels of two isostructural In-MOFs with distinct pore environments, and the resulting $Ru(bpy)_2(dppz)$@In-MOFs were utilized as highly recyclable heterogeneous visible-light photoredox catalysts.

Visible-light photosensitizers are key components in a wide range of photon-driven applications, including light harvesting and photocatalysis.[1-4] Among them, cationic Ru(II) polypyridine complexes have emerged as particularly popular sensitizers due to their long-lived photoexcited triplet metal-to-ligand charge transfer (^{3}MLCT) states.[2-4] One of the most extensively studied examples is $[Ru(bpy)_3]^{2+}$ (bpy = 2,2′-bipyridine). Upon excitation at 452 nm, the photoexcited $^*[Ru(bpy)_3]^{2+}$ exhibits intense photoluminescence (PL) centered at 615 nm, with an excited-state lifetime of approximately 1100 ns in acetonitrile at room temperature.[3] This long PL lifetime makes $[Ru(bpy)_3]^{2+}$ a highly versatile sensitizer for numerous applications. Among these, visible-light photoredox catalysis has recently flourished as a powerful platform for efficient organic transformations. Several excellent review articles have highlighted the effectiveness of $[Ru(bpy)_3]^{2+}$ as a photoredox catalyst (PC) in diverse and synthetically important reactions.[2,3] Interestingly, the photoexcited $^*[Ru(bpy)_3]^{2+}$ possesses substantial redox potentials and is capable of acting as either an oxidant or a reductant, depending on the reaction conditions. Likewise, many other cationic Ru(II) polypyridine complexes have proven to be efficient PCs in various visible-light photoredox reactions conducted under mild conditions.[2,3]

Department of Chemistry and Protein Research Center for Bio-Industry, Hankuk University of Foreign Studies, Yongin 17035, Republic of Korea. E-mail: shuh@hufs.ac.kr; Fax: +82 31 330 4566; Tel: +82 31 330 4522

Electronic Supplementary Information (ESI) available: Experimental procedures, crystal structure and microscopic image, cyclic voltammograms, PXRD patterns, PL lifetimes and their components, redox potentials, catalysis results, and proposed reaction mechanisms. See DOI: 10.1039/x0xx00000x

†These authors contributed equally to this work.

The complex $[Ru(bpy)_2(dppz)]^{2+}$ (dppz = dipyrido[3,2-*a*:2′,3′-*c*]phenazine) is an important photochemical analogue of $[Ru(bpy)_3]^{2+}$, distinguished by the extended, planar, and electron-deficient dppz ligand. A hallmark of $[Ru(bpy)_2(dppz)]^{2+}$ is its strong DNA-intercalating ability, enabled by the large π-surface of the dppz ligand. In aqueous solution the complex is non-emissive, a consequence of hydrogen-bonding interactions between water molecules and the phenazine nitrogen atoms of dppz.[5] Upon intercalation between DNA base pairs, these quenching interactions are disrupted and the PL is restored, giving rise to the well-known 'DNA light switch' effect that underpins its applications in molecular sensing and bioimaging.

The PL behavior of $[Ru(bpy)_2(dppz)]^{2+}$ differs markedly from that of the homoleptic $[Ru(bpy)_3]^{2+}$ complex, which possesses a single low-lying ^{3}MLCT excited state. In contrast, $[Ru(bpy)_2(dppz)]^{2+}$ exhibits two distinct ^{3}MLCT states due to the π-extended nature of dppz: a higher-energy emissive $^3MLCT_{prox}$ state localized on the proximal bpy units and a lower-energy non-emissive (or weakly emissive) $^3MLCT_{dis}$ state localized on the distal phenazine portion of dppz.[6-8] The relative energies of these states are highly sensitive to their environment. A recent study showed that photoexcitation triggers a relatively slow electron transfer from the *Ru(II) center to the bpy portion of dppz, followed by a much faster intraligand electron transfer from bpy to the phenazine moiety (sub-70 fs), ultimately localizing the excited electron on the phenazine nitrogen atoms.[9] These unusual excited-state dynamics suggest that encapsulating $[Ru(bpy)_2(dppz)]^{2+}$ within metal–organic frameworks (MOFs) of differing pore environments may yield new tunable PL behaviors. Furthermore, despite the widespread application of Ru(II) polypyridine complexes in photoredox catalysis, the specific activity of $[Ru(bpy)_2(dppz)]^{2+}$ has received surprisingly little attention.

In this study, we report the preparation of two new heterogenized visible-light PCs, $Ru(bpy)_2(dppz)$@InBTB and $Ru(bpy)_2(dppz)$@InTATB, by encapsulating $[Ru(bpy)_2(dppz)]^{2+}$ within two isostructural anionic MOFs—InBTB and InTATB

View Article Online
DOI: 10.1039/D6DT00489J

(where H_3BTB = 1,3,5-benzenetribenzoic acid and H_3TATB = 4,4′,4″-*s*-triazine-2,4,6-triyltribenzoic acid, see Fig. S1)—which possess large channels and distinct pore environments: electron-donating vs. electron-accepting groups of the tritopic bridging ligands. The solid-state PL properties of these hybrid materials were investigated using steady-state fluorescence spectroscopy, while their PL lifetimes were analyzed by time-resolved photoluminescence (TRPL) and fluorescence lifetime imaging microscopy (FLIM). The redox potentials of each heterogenized photosensitizer were estimated using cyclic voltammetry (CV) and fluorescence spectroscopy. Finally, their visible-light photoredox catalytic activities were evaluated for the aza-Henry reaction of 2-phenyl-1,2,3,4-tetrahydroisoquinoline (THIQ) and for the aerobic oxidation of benzyl halides under compact fluorescent lamp (CFL) irradiation at room temperature.

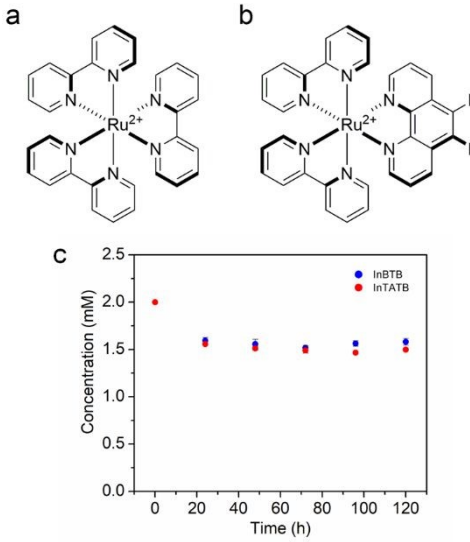

Fig. 1 The structural comparison of (a) $[Ru(bpy)_3]^{2+}$ and (b) $[Ru(bpy)_2(dppz)]^{2+}$. (c) Time-dependent encapsulation profiles of $[Ru(bpy)_2(dppz)]^{2+}$ by the as-prepared InBTB and InTATB in acetonitrile. Each measurement was repeated in triplicate.

The molecular dimension of $[Ru(bpy)_2(dppz)]^{2+}$ is much larger than $[Ru(bpy)_3]^{2+}$ due to the long flat geometry of the dppz ligand compared to bpy ligand as depicted in Fig. 1a and 1b. Therefore, MOFs with sufficiently large channel dimensions are mandatory to encapsulate $[Ru(bpy)_2(dppz)]^{2+}$ to successfully produce heterogenized $Ru(bpy)_2(dppz)$@MOF PC systems. The anionic InBTB was chosen as the encapsulation host material because InBTB contains pores large enough to encapsulate $[RuL_3]^{2+}$ (L = bpy, phen, and bpz), rhodamine 6G (Rh6G), and Reichardt's dye (RD) without any difficulties.[10-12] InBTB and InTATB exhibit isostructural frameworks with identical topologies, owing to their structurally similar tritopic linkers. Their doubly-interpenetrated 3D frameworks feature intricate pore geometries with oval-shaped cross-sections. The pore dimension of InTATB was previously investigated by Cao et al. by using N_2 gas sorption analysis at 77 K.[13] Considering the pore dimensions (mostly 1.1 nm, up to 1.6 nm) and the molecular size of $[Ru(bpy)_2(dppz)]^{2+}$ complex (1.1–1.7 nm),[14] the complex ion is suitably sized for encapsulation. Its asymmetric shape, featuring a protruding planar moiety, further facilitates its incorporation into the In-MOFs.

Gentle shaking of acetonitrile solution of $[Ru(bpy)_2(dppz)][BF_4]_2$ with InBTB crystals produced red color crystals after 5 d (Fig. S2). This characteristic red color indicates the possible encapsulation of $[Ru(bpy)_2(dppz)]^{2+}$ through a simple cation-exchange process. Stimulated from this promising preliminary result, the encapsution of $[Ru(bpy)_2(dppz)]^{2+}$ within the isostructural channels of InTATB was also investigated. The InTATB, or $(Et_4N)_3[In_3(TATB)_4]\cdot(DEF)_{16}\cdot(H_2O)_{11}$,[13,15] is an isostructural MOF with InBTB having an anionic framework with a tritopic $TATB^{3-}$ bridging linker instead of BTB^{3-} linker (Fig. S3, DEF = *N*,*N*-diethylformamide). As a result, InTATB is considered to possess a more electron-deficient pore environment compared to InBTB, where the central phenyl ring of the BTB^{3-} linker renders the environment electron-rich. The time-dependent encapsulation amounts of $[Ru(bpy)_2(dppz)]^{2+}$ investigated by UV-Vis spectroscopy is depicted in Fig. 1c. The encapsulation process was almost finished after 1 d like other previous systems.[10,15] The difference in encapsulation amounts is not significant between InBTB (0.42 μmol/mg-solids) and InTATB (0.5 μmol/mg-solids). These amounts are very comparable or more than the previous data of RuL_3@InBTB (0.33 – 0.42 μmol/mg-solids) where L = bpy, phen, and bpz.[10] Thus, the large $[Ru(bpy)_2(dppz)]^{2+}$ complex ion does not have difficulty in being encapsulated within the channels of both In-MOFs.

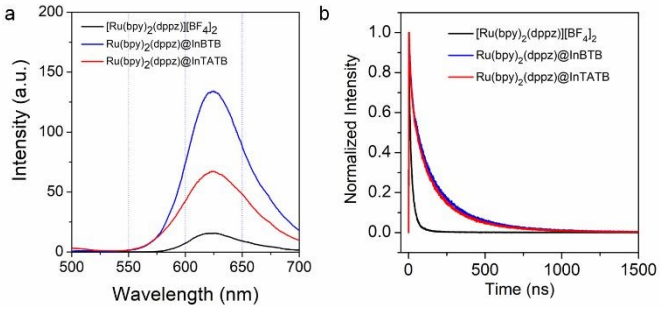

Fig. 2 (a) Solid-state PL spectra of crystalline $[Ru(bpy)_2(dppz)][BF_4]_2$, $Ru(bpy)_2(dppz)$@InBTB, and $Ru(bpy)_2(dppz)$@InTATB. All spectra were obtained at the excitation of 450 nm. (b) Normalized solid-state PL decay curves for free $[Ru(bpy)_2(dppz)][BF_4]_2$, $Ru(bpy)_2(dppz)$@InBTB, and $Ru(bpy)_2(dppz)$@InTATB.

As shown in Fig. S4, the PXRD patterns of both MOF samples consist of broad features, which are indicative of decreased crystallinity following guest encapsulation. We have consistently observed that the encapsulation of cationic guest ions within InBTB and InTATB, using ethanol or acetonitrile, tends to decrease the intensity of PXRD diffraction peaks.[10-12,15] Such behavior likely stems from the replacement of original DEF and water molecules with ethanol or acetonitrile, resulting in broadened signals and reduced peak heights. Nevertheless, we were previously able to determine the crystal structures for a series of RuL_3@InBTB and dye@InBTB.[10-12] Furthermore, as shown in Fig. S2, the optical microscopic images of both $Ru(bpy)_2(dppz)$@InBTB and $Ru(bpy)_2(dppz)$@InTATB confirm that the framework integrity is maintained.

The PL emission characteristics of $Ru(bpy)_2(dppz)$@InBTB and $Ru(bpy)_2(dppz)$@InTATB were investigated by using steady-

state fluorescence spectroscopy in solid state. The PL spectra is shown in Fig. 2a. The structural confinement within pre-organized MOF channels often induces specific spatial distributions and orientations of the guest ions. Accordingly, the PL properties of the encapsulated dyes or Ru(II) polypyridine complexes tend to differ from those of free crystalline states due to the confinement effects which effectively isolate each guest ion and minimize the non-radiative decay pathways for excited state of each guest ion.[10-12,15] Previous study also indicated that the encapsulated Ru(II) polypyridine $[RuL_3]^{2+}$ (L = bpy, phen, and bpz) ions exhibited distinct solid-state PL emissions compared to their free ions due to confinement effects in the nanoscopic channels of isostructural InBTB and InTATB.[10,15] Notably, crystal structure analyses of RuL_3@InBTB reveal that each Ru(II) polypyridine complex engages in unique hydrogen-bonding interactions with the host framework, highlighting the sensitivity of their excited state properties to local microenvironments.[10] As in Fig. 2a, the PL emission spectra clearly indicate that $[Ru(bpy)_2(dppz)]^{2+}$ encapsulated in InBTB has large enhancement of PL intensity compared to the crystalline solids of $[Ru(bpy)_2(dppz)][BF_4]_2$.[16] This observation can be attributed to the suppression of the self-quenching effect in the bulk crystalline state and the effective restriction of other non-radiative decay pathways. Despite the difference in intensity, the emission maxima of the two samples are nearly identical, appearing at 625 and 627 nm for $Ru(bpy)_2(dppz)$@InBTB and $[Ru(bpy)_2(dppz)][BF_4]_2$, respectively, under the same excitation wavelength (λ_{ex} = 450 nm). Additionally, $Ru(bpy)_2(dppz)$@InTATB displayed a significantly enhanced emission intensity compared to the free complex $[Ru(bpy)_2(dppz)][BF_4]_2$. The central electron-accepting *s*-triazine ring of the $TATB^{3-}$ linker may slightly diminish the quantum yield, leading to a lower PL emission intensity compared to that of $Ru(bpy)_2(dppz)$@InBTB. Nonetheless, the PL maximum (λ_{max} = 623 nm) remains essentially unchanged.

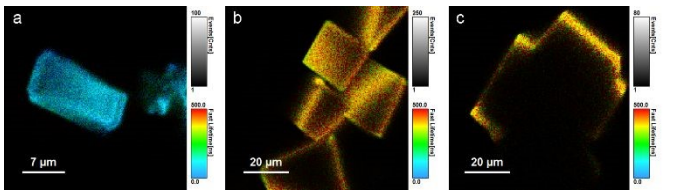

Fig. 3 Fluorescence lifetime imaging (FLIM) images of (a) crystalline $[Ru(bpy)_2(dppz)][BF_4]_2$, (b) $Ru(bpy)_2(dppz)$@InBTB, and (c) $Ru(bpy)_2(dppz)$@InTATB.

The PL lifetime of the excited state PC is one of the governing factors for its photoredox catalytic activities. The TRPL decay curves (Fig. 2b) were measured to compare the excited state lifetimes of the encapsulated $[Ru(bpy)_2(dppz)]^{2+}$ species compared to free crystsalline solids as summarized in Table S1 and Table S2. The PL lifetime of $Ru(bpy)_2(dppz)$@InBTB (270 ns) is much longer than free solids of $[Ru(bpy)_2(dppz)][BF_4]_2$ (21 ns). More than 10-fold enhancement was observed. $Ru(bpy)_2(dppz)$@InTATB exhibited a slightly shorter lifetime (254 ns) than $Ru(bpy)_2(dppz)$@InBTB. In this instance, however, the contrasting pore environments of InTATB and InBTB did not result in a pronounced difference in the lifetimes of the encapsulated complexes, in contrast to previously reported cases involving $[RuL_3]^{2+}$ (L = bpy, phen, and phen).[10,15] Furthermore, $Ru(bpy)_2(dppz)$@InBTB displayed a marginally longer lifetime than its InTATB counterpart, as evidenced by its slightly higher value relative to the 254 ns observed for the latter. This result may be attributable to the less effective intermolecular π···π interactions between the very bulky dppz ligand and the electron-donating central phenyl group of BTB^{3-} or electron-accepting central *s*-triazine moiety of $TATB^{3-}$ linkers. Although we are unable to give a plausible explanation of this phenomenon more in detail due to the lack of crystal structures of $Ru(bpy)_2(dppz)$@In-MOFs, the bulkier $[Ru(bpy)_2(dppz)]^{2+}$ complex should have distinct interactions with the anionic frameworks compared to smaller $[RuL_3]^{2+}$ (L = bpy, phen, and phen) complexes. While the PL lifetimes of $Ru(bpy)_2(dppz)$@InBTB and $Ru(bpy)_2(dppz)$@InTATB are shorter than $Ru(bpy)_3$@InBTB (402 ns) and $Ru(bpy)_3$@InTATB (499 ns), they are longer than $Ru(bpz)_3$@InBTB (96 ns) and $Ru(bpz)_3$@InTATB (110 ns) despite the very similar values of free crystalline solids of $[Ru(bpy)_2(dppz)][BF_4]_2$ and $[Ru(bpz)_3][PF_6]_2$. The PL lifetime of crystalline $[Ru(bpz)_3][PF_6]_2$ is 19 ns.[10] Fluorescence lifetime imaging (FLIM) images are shown in Fig. 3, and the observed lifetimes from FLIM are consistent with the measured lifetimes.

The redox potential of a PC is a decisive factor determining its catalytic feasibility in photoredox reactions.[17] In this context, the redox potentials of the encapsulated $[Ru(bpy)_2(dppz)]^{2+}$ in $Ru(bpy)_2(dppz)$@InBTB and $Ru(bpy)_2(dppz)$@InTATB were estimated from CV and PL emission spectroscopy. The CV curves for $[Ru(bpy)_2(dppz)]^{2+}$, $Ru(bpy)_2(dppz)$@InBTB, and $Ru(bpy)_2(dppz)$@InTATB are shown in Figs. S5 and S6. The resulting redox potentials are summarized in Table S3 and Fig. S7. The redox potentials of $Ru(bpy)_2(dppz)$@InBTB and $Ru(bpy)_2(dppz)$@InTATB shifted slightly relative to the free $[Ru(bpy)_2(dppz)]^{2+}$ complex measured in acetonitrile. The half-wave reduction and oxidation potentials of free $[Ru(bpy)_2(dppz)]^{2+}$ are –0.97 and +1.29 V (vs. SCE) in acetonitrile at room temperature. The corresponding potentials are –0.85 and +1.31 V for $Ru(bpy)_2(dppz)$@InBTB, and –0.85 and +1.31 V for $Ru(bpy)_2(dppz)$@InTATB. Thus, encapsulation within InBTB or InTATB does not significantly alter the intrinsic redox properties of $[Ru(bpy)_2(dppz)]^{2+}$. Similar behaviour has been reported for RuL_3@InBTB and RuL_3@InTATB (L = bpy, phen, and bpz).[10,15] While the ground state reduction potentials of $Ru(bpy)_2(dppz)$@InBTB and $Ru(bpy)_2(dppz)$@InTATB are higher than those of previously reported $Ru(bpy)_3$@In-MOF analogues, their ground state oxidation potentials are comparable to those of the latter.[15] The excited state redox potentials of the encapsulated $[Ru(bpy)_2(dppz)]^{2+}$ suggest that both $Ru(bpy)_2(dppz)$@InBTB and $Ru(bpy)_2(dppz)$@InTATB can act as either oxidants or reductants under appropriate conditions. Notably, the excited state reduction potentials of $Ru(bpy)_2(dppz)$@InBTB (+1.17 V) and $Ru(bpy)_2(dppz)$@InTATB (+1.17 V) are much higher than those of $Ru(bpy)_3$@InBTB (+0.80 V) and $Ru(bpy)_3$@InTATB (+0.75 V).[15] These excited state reduction potentials fall between those of [

View Article Online DOI: 10.1039/D6DT01429J

$Ir(dF(CF_3)ppy)_2(dtbpy)]^{3+}$ ($^*Ir(III)/Ir(II)$ = +1.21 V; $dF(CF_3)ppy$ = 2-(2,4-difluorophenyl)-5-(trifluoromethyl)pyridine and dtbpy = 4,4'-di-*tert*-butyl-2,2'-bipyridine) and $[Ru(bpm)_3]^{2+}$ ($^*Ru(II)/Ru(I)$ = +0.99 V; bpm = 2,2′-bipyrimidine).[3]

Photolytically catalyzed aza-Henry reaction is a straightforward synthetic strategy to prepare β-nitroamines through the addition of a nitroalkane to an imine.[3,18] It has also been proven that the aza-Henry reaction between 2-phenyl-1,2,3,4-tetrahydroisoquinoline (THIQ) and nitromethane under visible light at room temperature is a good model photoredox reaction for both homogeneous and heterogeneous Ru(II) polypyridine-based PCs acting as a single electron-transfer (SET) photocatalyst under visible light irradiation. In our recent study, we demonstrated the effective photoredox catalytic activities of heterogeneous RuL_3@InBTB and RuL_3@InTATB (L = bpy, phen, and bpz) in the aerobic aza-Henry reaction of THIQ at room temperature.[10,15] Notably, RuL_3@InTATB exhibited higher product yields and selectivity compared to RuL_3@InBTB despite the isostructural frameworks of anionic InBTB and InTATB. The superior catalytic activity of RuL_3@InTATB compared to RuL_3@InBTB is primarily attributed to the electron-accepting nature of the *s*-triazine moieties within the InTATB pore environment.[15] In particular, the aza-Henry reaction of THIQ is significantly facilitated by $Ru(bpy)_3$@InTATB due to the electron-accepting functionality of the *s*-triazine unit within the $TATB^{3-}$ linker. This feature extends the PL lifetime compared to $Ru(bpy)_3$@InBTB, which is attributed to enhanced electronic communication facilitated by intermolecular π···π interactions between the bpy ligand and the $TATB^{3-}$ linker, ultimately boosting overall photocatalytic efficiency. In $Ru(bpy)_3$@InBTB case, there is an electron-donating central phenyl moiety in BTB^{3-} linker.

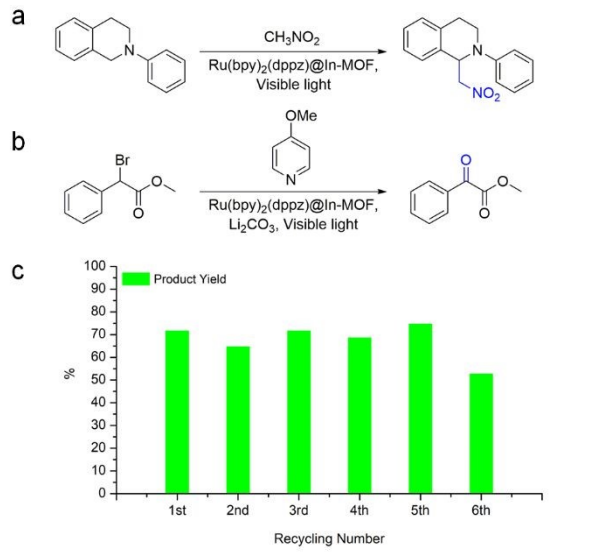

Fig. 4 The aza-Henry reaction of THIQ with nitromethane (a) and aerobic oxidation of methyl α-bromophenylacetate (b) catalyzed by $Ru(bpy)_2(dppz)$@In-MOFs visible-light photoredox catalytic systems in air. (c) Recyclability of $Ru(bpy)_2(dppz)$@InTATB in the aza-Henry reaction of THIQ.

The catalytic activity of $Ru(bpy)_2(dppz)$@InBTB and $Ru(bpy)_2(dppz)$@InTATB were also investigated using the aza-Henry reaction of THIQ. The previously proposed reaction mechanism is shown in Fig. S8.[3,15] The reaction proceeds via a reductive quenching pathway of the photoexcited Ru(II) complex, where a SET occurs from the THIQ substrate to the excited species. This mechanism is further supported by the high excited state reduction potentials observed for both $Ru(bpy)_2(dppz)$@InBTB and $Ru(bpy)_2(dppz)$@InTATB. The respective desired product yields are 62 and 72 % for $Ru(bpy)_2(dppz)$@InBTB and $Ru(bpy)_2(dppz)$@InTATB. These results correspond to turnover numbers (TONs) of 31 and 36, respectively. These moderately high product yields unequivocally confirm that the heterogenized $[Ru(bpy)_2(dppz)]^{2+}$ ion is an also good PC for aza-Henry reaction under mild reaction conditions. Unlike the previous $Ru(bpy)_3$@InBTB and $Ru(bpy)_3$@InTATB systems,[15] the catalytic yield of $Ru(bpy)_2(dppz)$@InTATB showed a relatively modest enhancement compared to $Ru(bpy)_2(dppz)$@InBTB. This indicates that the influence of the *s*-triazine linker varies depending on the specific Ru(II) complex encapsulated. Although the crystal structures of $Ru(bpy)_2(dppz)$@InBTB and $Ru(bpy)_2(dppz)$@InTATB could not be solved, the distinct intermolecular interactions between the encapsulated $[Ru(bpy)_2(dppz)]^{2+}$ ion and the anionic frameworks may affect the catalytic activities. As shown in the images in Fig. S9, the reaction mixture was observed before and after the aza-Henry reaction using $Ru(bpy)_2(dppz)$@InTATB. The reaction mixture slightly darkened from its initially colorless state. This color change likely results from the formation of the red-colored iminium ion intermediate from the THIQ substrate.[10] Notably, the red catalyst particles remained morphologically intact throughout the process.

To further investigate, we evaluated the photoredox catalytic activity of the free $[Ru(bpy)_2(dppz)]^{2+}$ complex in acetonitrile under identical reaction conditions. Surprisingly, the free complex exhibited significantly lower activity, with a product yield of approximately 41%. Comparing this to a previously reported control test without a catalyst,[10] $[Ru(bpy)_2(dppz)]^{2+}$ complex showed no appreciable enhancement in yield. This suggests that the free complex alone may lack effective photoredox catalytic activity for the aza-Henry reaction in acetonitrile under aerobic conditions. Further investigation into the substrate scope and reaction diversity of this catalytic system is planned.

One of the most important advantages of the encapsulation of $[Ru(bpy)_2(dppz)]^{2+}$ ion lies in its heterogenization for recyclable catalysis. It was anticipated that the strong encapsulation of the large divalent cationic $[Ru(bpy)_2(dppz)]^{2+}$ ion within the ionic MOF channels would lead to excellent recycling performance. In this sense, $Ru(bpy)_2(dppz)$@InTATB was selected for catalyst recycling experiment. $Ru(bpy)_2(dppz)$@InTATB revealed remarkable recycling activity during six consecutive aza-Henry reactions. The product yield maintained its original activity up to fifth recycling (65~75%) and slightly decreased at sixth reaction (53%) as shown in Fig. 4c. These data clearly show that $Ru(bpy)_2(dppz)$@InTATB is a robust heterogeneous catalyst system. It is noteworthy that the $Ru(bpy)_2(dppz)$@InTATB sample, stored in a screw-capped vial at ambient conditions in a desiccator for over a year,

showed consistent catalytic activity and recyclability. Consequently, encapsulating the $[Ru(bpy)_2(dppz)]^{2+}$ complex within In-MOFs not only enhances its catalytic performance but also improves its recyclability.

The catalytic activities of $Ru(bpy)_2(dppz)$@InBTB and $Ru(bpy)_2(dppz)$@InTATB were also investigated by using the aerobic oxidation of benzyl halides to produce α-aryl carbonyl derivatives (Fig. S10).[19] Five different benzyl halides were selected for reaction under visible light irradiation at room temperature. In these cases, the catalytic activity differences between $Ru(bpy)_2(dppz)$@InBTB and $Ru(bpy)_2(dppz)$@InTATB are not significant as shown in Table S4. Both product yields and selectivity for two catalytic systems are similar each other. The product yields of $Ru(bpy)_2(dppz)$@InBTB (66~85 %) are not significantly different from those of $Ru(bpy)_2(dppz)$@InTATB (60~90%). These results are different from the observations that $Ru(bpy)_2(dppz)$@InTATB showed better product yield over $Ru(bpy)_2(dppz)$@InBTB in the aza-Henry reaction.

In conclusion, the large cationic complex $[Ru(bpy)_2(dppz)]^{2+}$ was successfully encapsulated within the channels of two isostructural anionic In-MOFs, InBTB and InTATB, which possess distinct pore environments, to yield $Ru(bpy)_2(dppz)$@InBTB and $Ru(bpy)_2(dppz)$@InTATB via a cation-exchange method. Both $Ru(bpy)_2(dppz)$@InBTB and $Ru(bpy)_2(dppz)$@InTATB exhibited greatly enhanced PL emission intensity in the solid state compared with free crystalline $[Ru(bpy)_2(dppz)][BF_4]_2$. The encapsulated complexes also showed prolonged excited-state PL lifetimes, attributed to confinement effects within the MOF frameworks. The visible-light photoredox catalytic activities of the two heterogenized systems were evaluated for the aza-Henry reaction of THIQ and for the aerobic oxidation of benzyl halides at room temperature. While $Ru(bpy)_2(dppz)$@InTATB showed a marginally higher yield than $Ru(bpy)_2(dppz)$@InBTB in the aza-Henry reaction, both catalysts exhibited varying photoredox activities in the aerobic oxidation of benzyl halides depending on the substrate. No consistent trends or systematic differences were observed in the latter, despite the distinct pore environments of the host frameworks. The $Ru(bpy)_2(dppz)$@InTATB demonstrated excellent recyclability, retaining most of its catalytic activity over six consecutive aza-Henry reaction cycles, with only a slight decrease in reactivity observed in the sixth run.

Author contributions

Jongseo Kim: Investigation, Data curation, Validation, Visualization. **Chan Gu Kim**: Investigation, Data curation, Validation. **Juwon Lee**: Investigation, Data curation, Validation. **Seong Huh**: Conceptualization, Methodology, Validation, Data curation, Writing – original draft, Writing – review & editing, Visualization, Supervision, Project administration, Funding acquisition.

Conflicts of interest

There are no conflicts to declare.

Data availability

View Article Online
DOI: 10.1039/D6DT00489J

The data supporting this article have been included as part of the SI: experimental procedures, crystal structure and microscopic image, PL lifetimes and their components, redox potentials, catalysis results, and proposed reaction mechanisms.

Acknowledgements

This work was supported by grants (2022R1F1A1063615) of the Basic Science Research Program through the National Research Foundation (NRF) funded by the Ministry of Education, Science and Technology, Republic of Korea. This work was also supported by the Hankuk University of Foreign Studies Research Fund of 2025.

Notes and references

1 P. D. Frischmann, K. Mahata and F. Würthner, *Chem. Soc. Rev.*, 2013, **42**, 1847–1870.
2 J. M. R. Narayanam and C. R. J. Stephenson, *Chem. Soc. Rev.*, 2011, **40**, 102–113.
3 C. K. Prier, D. A. Rankic and D. W. C. MacMillan, *Chem. Rev.*, 2013, **113**, 5322−5363.
4 W. Nam, Y.-M. Lee and S. Fukuzumi, *Bull. Korean Chem. Soc.*, 2024, **45**, 503–519.
5 A. E. Friedman, J.-C. Chambron, J.-P. Sauvage, N. J. Turro and J. K. Barton, *J. Am. Chem. Soc.*, 1990, **112**, 4960–4962.
6 B. Önfelt, P. Lincoln and B. Nordén, *J. Am. Chem. Soc.*, 2001, **123**, 3630–3637.
7 B. Önfelt, J. Olofsson, P. Lincoln and B. Nordén, *J. Phys. Chem. A*, 2003, **107**, 1000–1009.
8 Y. Sun, S. N. Collins, L. E. Joyce and C. Turro, *Inorg. Chem.*, 2010, **49**, 4257–4262.
9 E. S. Ryland, X. Yang, D. Garratt, W. C. Henke, A. Kahraman, M. Taub, M. Sachs, E. Biasin, C. Y. Hampton, D. J. Hoffman, G. Coslovich, K. Kunnus, G. L. Dakovski, M. W. Mara, L. X. Chen, K. L. Mulfort, X. Li and A. A. Cordones, *Angew. Chem. Int. Ed.*, 2025, **64**, e202509496.
10 I.-H. Choi, S. Yoon, S. Huh, S.-J. Kim and Y. Kim, *Chem. Eur. J.*, 2020, **26**, 14580–14584.
11 I.-H. Choi, S. B. Yoon, S. Huh, S.-J. Kim and Y. Kim, *Sci. Rep.*, 2018, **8**, 9838.
12 E.-Y. Cho, J.-M. Gu, I.-H. Choi, W.-S. Kim, Y.-K. Hwang, S. Huh, S.-J. Kim and Y. Kim, *Cryst. Growth Des.*, 2014, **14**, 5026−5033.
13 Y. Huang, Z. Lin, H. Fu, F. Wang, M. Shen, X. Wang and R. Cao, *ChemSusChem*, 2014, **7**, 2647–2653.
14 H. Song, J. T. Kaiser and J. K. Barton, *Nat. Chem.*, 2012, **4**, 615–620.
15 J. Kim and S. Huh, *Dalton Trans.*, 2025, **54**, 14322–14330.
16 E. Amouyal, A. Homsi, J.-C. Chambron and J.-P. Sauvage, *J. Chem. Soc. Dalton Trans.*, 1990, 1841–1845.
17 T. Bortolato, S. Cuadros, G. Simionato and L. Dell'Amico, *Chem. Commun.*, 2022, **58**, 1263–1283.
18 V. K. Patel, D. P. Patel and S. K. Singh, *Tetrahedron*, 2025, **185**, 134803.
19 Yijin Su, Liangren Zhang and Ning Jiao, *Org. Lett.*, 2011, **13**, 2168–2171.

View Article Online
DOI: 10.1039/D6DT00489J

Data availability statements

$[Ru(bpy)_2(dppz)]^{2+}$ encapsulated isostructural In-MOFs: a comparative study of their photoluminescence and photoredox catalytic activities

Jongseo Kim, Chan Gu Kim, Juwon Lee and Seong Huh*

The data supporting this article have been included as part of the SI: experimental procedures, crystal structure and microscopic image, PL lifetimes and their components, redox potentials, catalysis results, and proposed reaction mechanisms.